EFFECT OF ENVIRONMENT AND MICROSTRUCTURE ON THE HIGH TEMPERATURE BEHAVIOR OF ALLOY 718

E. Andrieu*, R. Cozar** and A. Pineau*
* Centre des Matériaux, Ecole des Mines, B.P.87, 91003 Evry Cédex, URA CNRS D0866, France
**Centre de Recherches, Aciéries d'Imphy, 58160 Imphy, France

Abstract

This paper is concerned with the micromechanisms and the metallurgical factors controlling the high temperature behavior of Alloy 718. The presentation is divided into two parts. In the first one the micromechanisms responsible for the transition in the fracture mode from transgranular to intergranular are reviewed. Two interrelated mechanisms are discussed : (i) slip-induced intergranular cracking and (ii) oxidation-assisted crack growth. A strong emphasis is laid upon the later one. Results of Auger spectrometry showing the formation of two types of oxides : a spinel type (Ni, Fe, O) and Cr_2O_3 oxide, are given. These results are used to discuss transient effects in crack growth behavior reported in the literature and the effect of hold time at minimun load observed during fatigue crack growth measurements. The second part of the paper deals with the study of metallurgical factors which control the elevated temperature resistance of Alloy 718. The effects of both heat treatment and compositional modifications on the strength and thermal stability are discussed. The requirements (composition, heat-treatment) to achieve a compact morphology consisting of cube shaped γ' precipitates covered on there six faces by γ" precipitates are given. A number of factors controlling more specifically the grain boundary strength (grain size, grain boundary morphology and chemistry) are also reviewed and discussed.

Superalloy 718—Metallurgy and Applications
Edited by E.A. Loria
The Minerals, Metals & Materials Society, 1989

Introduction

This paper deals with a review of the micromechanisms responsible for the high temperature fatigue crack behavior of Alloy 718 as well as with the review of a number of metallurgical improvements which could be imposed to this material. The paper is divided into two main parts. The first part deals with the micromechanisms responsible for the transition in crack growth mode from transgranular to intergranular. In this part an attempt is made to analyze in some detail one mode of failure which is frequently observed in many Ni-base superalloys, i.e. oxidation-assisted crack growth. The second part is devoted to the study of a number of metallurgical factors leading to the improvement of thermal stability and the resistance to intergranular cracking. In this respect we will rely in the most part upon results obtained in our laboratory at Ecole des Mines on various heats of Alloy 718.

The fatigue crack growth rate (FCGR) behavior of Alloy 718 is reviewed in detail in his conference [1]. A number of results published in the literature are reported in Fig.1 and Table 1. Fig. 1 shows that, at room temperature, in the medium range of FCGR ($\simeq 10^{-4}$ to 10^{-3} mm/cycle) the results are not very sensitive to the details of the microstructure and test conditions. On the other hand, a large scatter band is observed when the results are obtained at an elevated temperature, especially when a hold time is imposed.

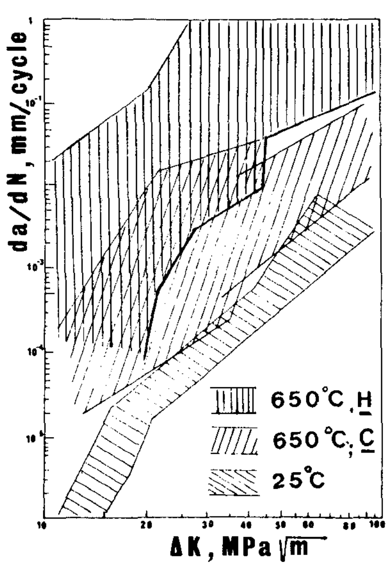

Figure 1 - Fatigue crack growth rate as a function of ΔK at 25°C and 650°C under continuous cycling (C) or with a hold time (H) (see Table 1).

Test	Frequency Hz	R.	Hold time, min	Ref.
20°C, continuous fatigue......	0.17	0	-	2
	2.5	0	-	3
	8.3	0.05	-	4
	10	0.05	-	5
	20	0.05	-	6
650°C, continuous fatigue....	5×10^{-2}	0.10	-	7
	5×10^{-2}	0.10	-	7
	0.17	0.05	-	8
	0.17	0.05	-	9
	0.67	0.05	-	4
	0.67	0.05	-	5
	20	0.10	-	7
	20	0.10	-	7
	20	0.10	-	7
650°C, fatigue with hold time...	0.17	0.05	0.1	8
	5×10^{-2}	0.10	0.167	7
	5×10^{-2}	0.10	0.167	7
	0.17	0.05	1	9
	0.17	0.05	1	8
	0.17	0.50	1	9
	5×10^{-2}	0.10	1	7
	5×10^{-2}	0.10	1	7
	5×10^{-2}	0.10	5	7
	0.17	0.05	10	8

Table 1 - Test conditions and reference.

The objective of this review is to provide some guidelines for the explanation of the occurrence of this scatter and to illustrate the degree of influence of both the microstructure and testing procedures. In this regard an acceptable explanation of the increase in high temperature FCGR is related to the accompanying fracture mode.

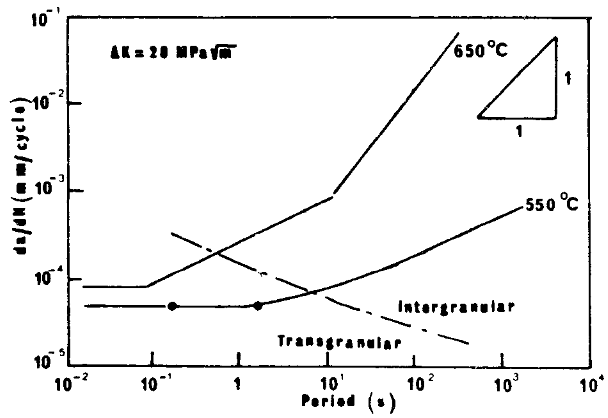

Figure 2 - Fatigue crack growth rate as a function of cycle period at 550°C and 650°C. Results obtained at $\Delta K = 20 MPa\sqrt{m}$. (Table 1).

Fig.2 assembles results published by several authors. Full details can be found elsewhere [10]. These results generally indicate that, under high frequency loading, the observed mode is transgranular. However, as the loading frequency decreases the fracture mode becomes intergranular leading to an increase in the FCGR. Under the latter condition, especially at 650°C and at low frequency the crack growth process is essentially time dependent. This raises the first question which is dealt with in the following section.

Mechanisms of intergranular cracking

The mechanisms of intergranular crack growth have been reviewed recently in Ref. [10-12]. They conclude that, for Alloy 718, tested below 650°C, two interactive mechanisms are considered prevalent : (i) slip induced intergranular cracking and (ii) oxidation-assisted crack growth. These mechanisms are described separately, although they are strongly interrelated.

Slip-induced intergranular cracking

At high strain amplitude, fatigue cracks in pure metals, such as Ni and Cu, nucleate preferentially along the grain boundaries at free surfaces. This mode of cracking also occurs in structural metals, specifically in Ni-base superalloys, at relatively low as well as at high temperatures. In a given material, such as pure Ni, it was shown recently [13-15] that the factors influencing this mode of cracking are : (i) the type of boundaries; (ii) the orientation of the grain boundaries with respect to the tensile axis and the free surface of the specimen and (iii) the slip character.

In Alloy 718 the slip character plays an important role in the development of intergranular cracking, as discussed earlier [6,16-18]. The slip character is related to the interactions between dislocations and the strengthening precipitates. This material is strengthened by the precipitates of two ordered phases, the simple cubic ($L1_2$) γ' phase and the γ'' phase which has a body-centered tetragonal structure. The dominant contribution to precipitation hardening arises from the latter phase. The deformation mechanisms, as well as the deformation microstructures pertaining to γ'' strengthened alloys have been studied in some detail (see e.g. [16-20]). In particular it was shown that the γ'' precipitates were sheared by dislocations and that cyclic plastic deformation proceeded by the propagation of planar bands of defects present both in the precipitates and in the matrix. These defects were identified as mechanical twins [16,20] . An example of these deformation twins is shown in Fig.3. In a more recent study devoted to the room temperature deformation modes of Alloy 718 it was confirmed that, when the size of γ'' particles exceeds a critical value ($\simeq$ 10 nm), these precipitates are sheared by the passage of deformation twins [21] . This study also showed that, for smaller precipitates, shearing occurs by the movement of groups of dislocations which enables restoration of order within the γ'' phase. At an elevated temperature ($\simeq$ 550°C), it was shown that a decrease in test frequency, or strain-rate, promoted the formation of mechanical twins. Fig.4 summarizes the results of detailed observations which were made both on smooth low cycle fatigue specimens and very close to the fracture surface of specimens used to measure the FCGR [6].

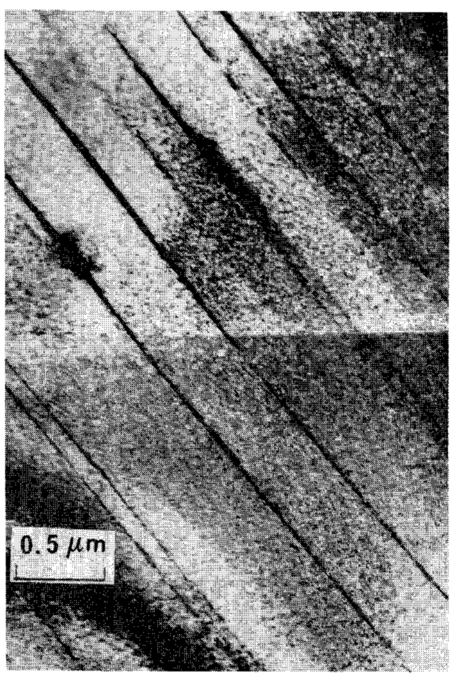

Figure - 3 Mechanical twins formed in a low cycle fatigue specimen ($\Delta\epsilon_p/2$= 0.56%, $\dot{\epsilon}$= $5.10^{-5}s^{-1}$)[16].

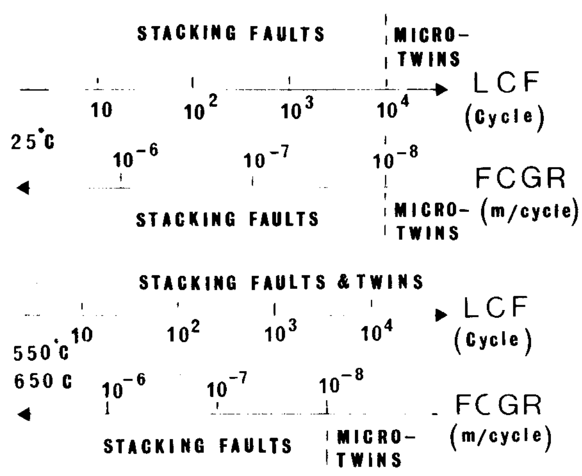

Figure 4 - Summary of the deformation modes observed both in LCF specimens and the vicinity of fatigue cracks [6].

The planar slip character and mechanical twinning exhibited in this material might, in part, account for the appearance of intergranular crack behaviour shown earlier (Fig.2), especially at intermediate temperature ($\simeq$550°C) when the detrimental effects of environment are not yet sufficiently pronounced. To illustrate this effect, FCGR tests were carried out both at 550°C and at 650°C under various wave-form signals [17]. The results are reported in Fig.5. It is observed that at 550°C the low frequency test (5.10^{-2}Hz) with continuous cycling leads to the highest FCGR as compared to the test performed at the same frequency but with a hold time of 10 s at both the minimum and maximum load. SEM observations showed that the slow strain-rate tests produced intergranular crack growth. This mode of failure is therefore reinforced by the conditions leading to abundant twinning. On the other hand, at 650°C, the hold time tests give rise to the largest FCGR. This does not mean that the deformation modes do not still play an important role but that their effect might have been hidden in part by the second mechanism related to oxidation which is discussed below.

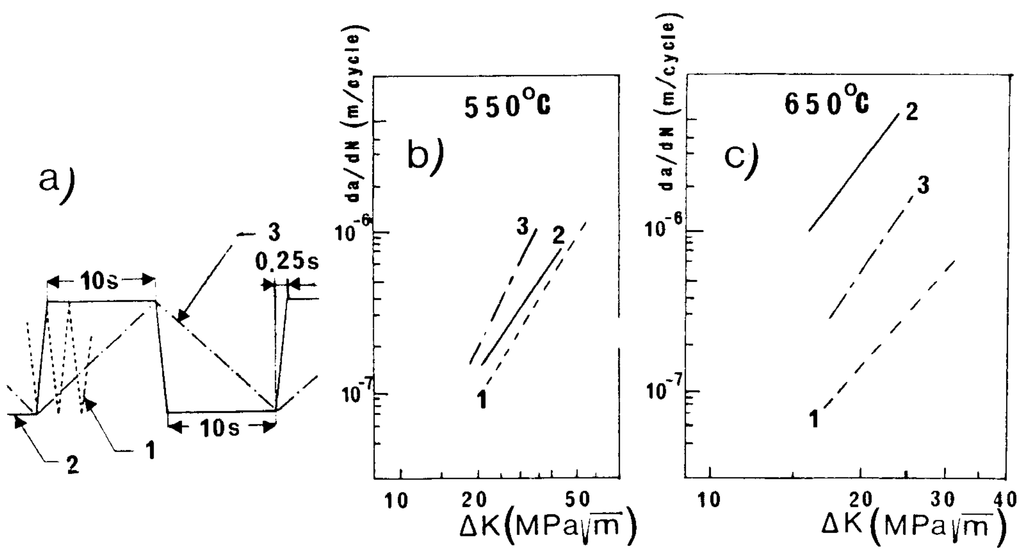

Figure 5 - Effect of wave-form signal (a) on the fatigue crack growth rate measured at 550°C (b) and 650°C (c) [17].

Oxidation-assisted crack growth

In Alloy 718 this form of damage is well documented but still very poorly understood. The first factor is the effect of partial oxygen pressure. Results obtained on one specific heat of Alloy 718 are given in Fig.6 [22] . Slow strain-rate tensile tests (load-line displacement rate of 0.5 mm/min) were carried out at 650°C on axisymmetrically precracked fatigue round bars. These tests were performed on a large grain Alloy 718 (≃ 150µm) in a chamber especially designed to investigate the effect of partial oxygen pressure. The results reported in Fig.6 show that the ratio of intergranular fracture, as measured on the fracture surface, increases with the increase in oxygen partial pressure. Under atmospheric pressure, 60% of the fracture surface of the test specimens was found to be intergranular while, under vacuum, the fracture mode was transgranular. There exists a transition in PO_2 between 10^{-3} Torr and 1 Torr below which the failure mode is fully transgranular. The detrimental effect of oxidation on the FCGR behavior is also well established [7,8]. Results obtained on another heat of Alloy 718 are given in Fig.7. These results were obtained in a study dealing with the effect of both environment (air versus vacuum)

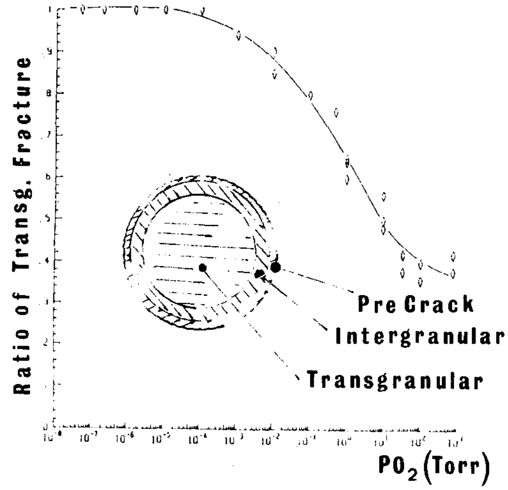

Figure 6 - Influence of partial oxygen PO_2 on intergranular fracture [22].

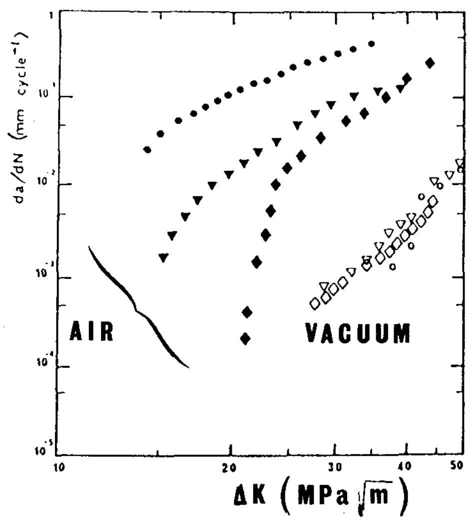

Figure 7 - Effect of environment on FCGR at 650°C (● ○ small grain size; ▼ ▽ large grain; ◆ ◇ necklace) [7].

and microstructure (large grain, small grain, necklace microstructure) on the FCGR behavior corresponding to a hold time of 5 mn at maximum load. It is concluded that the strong microstructural effects observed under air environment no longer exist when these various microstructures are tested under vacuum.

If the form of oxygen attack by simple absorption of oxygen at crack tip is not included, two other types of damage remain to be considered : (i) generalized oxidation or preferential grain boundary oxidation and (ii) internal oxidation. In the first case an oxide layer is formed at the crack tip and cracking occurs in this layer or at the matrix-oxide interface while, in the second case, oxygen diffuses into the metal ahead of the main crack and promotes the formation of subsurface cracks which are linked to the main crack. These two forms of damage have been discussed recently, [12] . The assumption that internal oxidation could take place in Alloy 718 tested around 650°C is still an open question. In the following we concentrate on the first form of oxidation damage. Fig.8 summarizes the results obtained in reference [22] , using AUGER spectrometry analysis to determine the types of oxide which were formed as a function of partial oxygen pressure and of specimen preparation. All the oxidation tests were performed at 650°C. The results reported in Fig.8 which were obtained on electropolished specimens show that, at low oxygen partial pressure ($\leqslant 10^{-4}$ Torr), only the protective Cr_2O_3 type oxide is formed. On the other hand, at higher oxygen partial pressure ($\geqslant 10^{-2}$Torr) both a spinel type

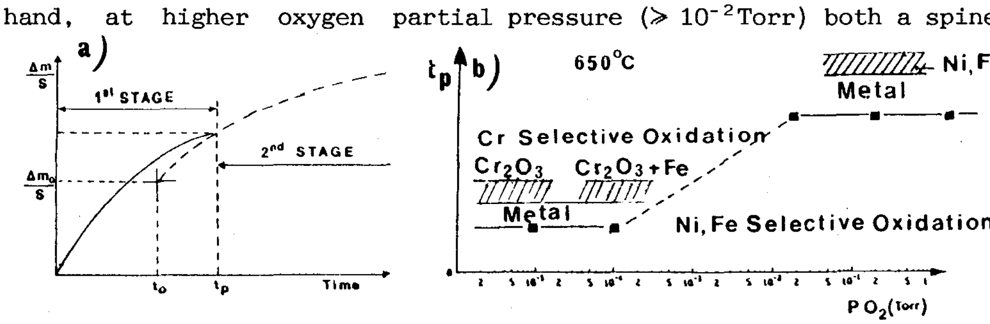

Figure 8 - Mechanism of oxidation as a function of time (a) and partial oxygen pressure (b) [22].

(NiFeO), which is not very protective, and Cr_2O_3 oxides are formed. This suggests that oxidation under air environment occurs in two stages, as indicated schematically in Fig.8a, with the formation of a Ni-Fe rich oxide followed by that of the more protective film formed by Cr_2O_3 oxide. The transition time, t_p, could not be measured as a function of PO_2. Under atmospheric pressure it was found to be of the order of a few minutes. The effect of predeformation was also studied by comparing the types of oxide formed either on the surface of polished specimens or on the surface of specimens which were previously given a shot-peening treatment. The results shown in Fig.9 indicate that, even at high PO_2, Cr_2O_3 oxide formation is promoted by a predeformation. This might have important consequences for in-service conditions since many components are systematically shot-peened. This mechanical treatment might prove beneficial not only for introducing compressive residual stresses but also for developing a more protective oxide film.

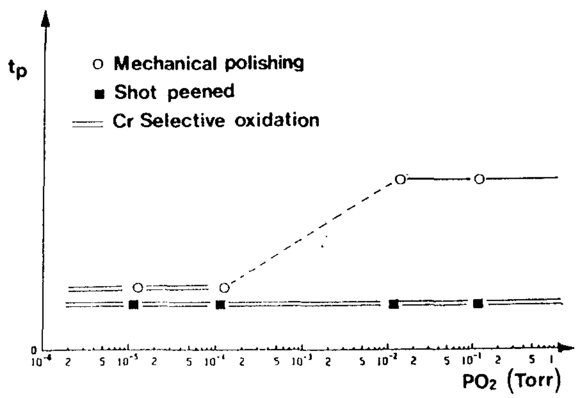

Figure 9 - Effect of specimen preparation and partial oxygen pressure on oxide formation [22].

As far as grain boudary oxidation is concerned, to the knowledge of the authors, no detailed results have been published. Fig.10 is a theoretical sketch based on the previous experimental results. It is assumed that grain boundary embrittlement is essentially due to short distance intergranular oxidation for exposure times lower than the transition time, t_p, corresponding to the formation of Cr rich oxide subscale. TEM studies are being undertaken to test this assumption. However even now there are results giving some credence to this theoretical sketch. In particular it was shown that a hold time applied at extremely low load,

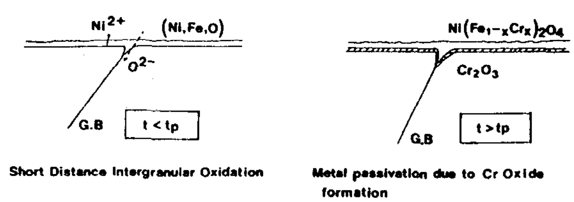

Figure 10 - Mechanism of grain boundary oxidation [22].

below the fatigue threshold, increased the FCGR measured at 650°C on one heat of Alloy 718 [23] . Theoretically such a hold time should not contribute to the "mechanical" crack growth. However the FCGR was found to be significantly increased even after a hold time as short as 30s. It was also observed that a saturation effect occurred for hold times longer than about 1000s. This time duration is of the same order of magnitude than the critical time, t_p, determined in the static oxidation study (Fig.8) and corresponding to the formation of Cr_2O_3 type oxide beneath the Ni-Fe rich oxide scale (Fig.10b). The saturation effect in FCGR behavior could therefore correspond to the formation of Cr_2O_3 oxide film.

A better understanding of these complex mechanisms is extremely important, not only for a better knowledge of the material, but also for very practical reasons, in particular the relevance of mechanical loading parameters. From the survey of the literature dealing with the high temperature behavior of Alloy 718 it is quite significant to notice that all the results of crack propagation rates measurements are reported using the stress intensity factor K as the relevant load geometry parameter. One of the authors of the present study has already mentionned the difficulties which could be found when the regime of crack growth rate is predominantly time-dependent [10]. It was shown earlier that the FCGR's measured in CT-type specimens containing different initial crack lengths were largely different at the same value of ΔK, the crack propagation rate being the largest for specimens with small crack lengths. More recently, in a study dealing with crack growth behavior under static loading it was also shown that both crack initiation and crack growth were largely dependent on load history effect [23] . This situation might be related to environmental effects. In the absence of a better understanding of these effects, very clear procedures must be adopted to determine the time-dependence of crack growth component.

To summarize, in addition to major compositional and metallurgical factors, discussed in the following section, intergranular cracking is controlled not only by the slip character but also, and essentially, by the detrimental effect of oxidation. This latter effect may in turn be responsible for the wide spread in the data shown in Fig.1.

Materials improvement in relation to microstructural modifications

This part is concerned with two aspects of the physical metallurgy of Alloy 718. The first one deals essentially with the effect of relatively large compositional changes on the phase stability of this material. The effect of varying Al,Ti and Nb content will be discussed. The second part is an attempt to review the metallurgical factors beneficial for the grain boundary resistance which, as discussed earlier, is a limiting factor for the use of this material.

Effect of heat treatment and compositional modifications on the strength and thermal stability of Alloy 718

Heat treatment. The precipitation hardening heat-treatment can significantly influence the high temperature resistance, especially the creep crack growth behavior. Wilson [24] showed that the rupture properties of Alloy 718 could largely be improved by a modification in heat-treatment giving larger precipitates. These results are shown in Fig.11 in addition to those obtained more recently [23]. The primary influence of overaging is to homogenize slip distribution within the grains which is favorable, as already discussed in the previous section. Fig.11 shows that the initial value of the stress intensity factor necessary to initiate and propagate a creep crack to failure is about twice the value determined in the material which has been conventionally heat treated.

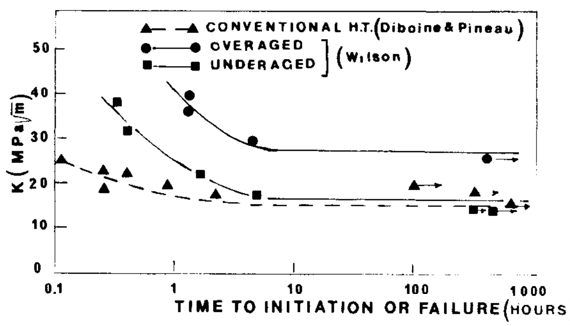

Figure 11 - Effect of heat treatment and initial stress intensity factor on time to initiation (Diboine and Pineau [23]) or time to failure (Wilson [24]).

Compositional modification. In addition to γ' (Ni_3TiAl) and γ" (Ni_3 Nb) metastable precipitates, Alloy 718 may also contain an incoherent, orthorhombic Ni and Nb rich phase which is the stable β phase. After annealing and thermomechanical treatment at relatively low temperature (≤ 980°C) this phase usually precipitates along the grain boundaries. The β phase precipitates also after extended times at elevated temperature to form particles which coarsen in a Widmenstätten-type shape. The metastable γ" particles are dissolved near the β-Ni_3 Nb laths; this is detrimental to the strength of the material [25]. Moreover the γ" ⟶ β phase transformation is largely accelerated by prior deformation, since it has been shown that planar defects present in the γ" particles after deformation can act as efficient nuclei for the precipitation of the stable β phase [16,26] . To minimize the driving force behind the β formation, a promising approach appears to point at modifying the alloy in the direction of a higher R = (Al + Ti) /Nb ratio. At present this ratio stands at approximately 0.7. Preliminary results obtained 15 years ago [25] showed that this approach was quite encouraging. More recently additional data has been published [27,28] showing that increasing the Al+Ti content in Alloy 718 could produce a more thermally and mechanically stable material.

A close control of the sequence of γ' and γ" precipitation reactions which are also directly related to Al, Ti and Nb content might also prove very useful to develop thermally stable precipitate microstructures. In conventional Alloy 718 (Ti+Al/Nb ≃ 0.7), γ" precipitates nucleate preferentially and coarsen on γ' particles. During overaging at elevated temperature this gives rise to microstructures similar to those shown in Fig.12 where relatively large DO_{22} disc shaped particles are observed to be tied up to smaller hemispherical γ' precipitates. On the other hand when both the chemical composition and the heat treatment were slightly modified it was shown earlier [25] that it was possible to develop a "compact morphology" which is very stable on prolonged aging. This morphology shown in Fig.13 consists of cube-shaped γ' particles coated on their six faces with a shell of γ" precipitates. One of the requirements to achieve this morphology is that the aging temperature has to be chosen in such a way that the initially isolated γ' precipitates reach a size of about 20 nm before the formation of γ" precipitates occurs (see Fig.14). Details of this morphology are described in Ref. [25].

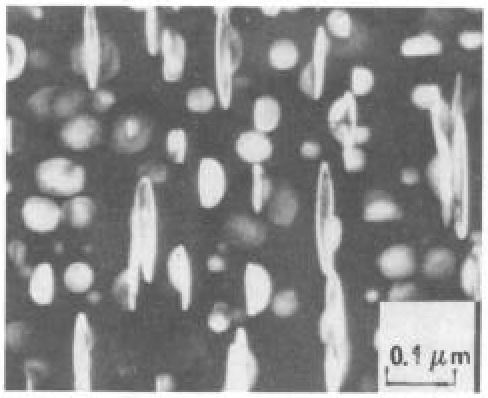

Figure 12 - Overaging of γ" precipitates observed by dark field TEM (Aging at 750°C for 128 hours) [25].

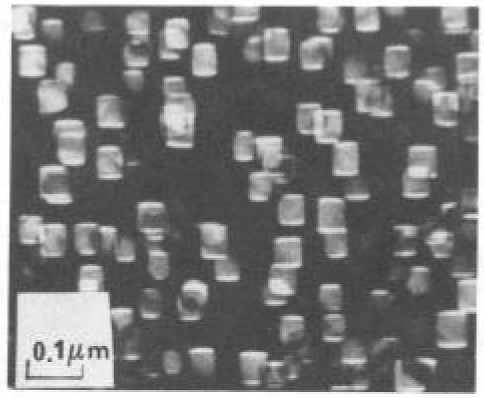

Figure 13 - Compact morphology observed in a modified composition by dark field electron microscopy. No overaging is noticed after 64 hours at 750°C [25].

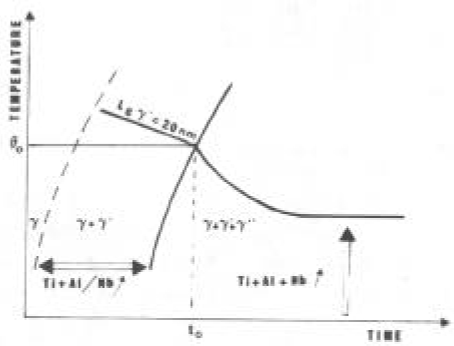

Figure 14 - Schematic TTT curves for the precipitation of γ' and γ" phases showing the existence of a critical temperature θ_o related to the critical γ' size, L_c [25] .

This preliminary study dealing with compositional changes was limited to S = Al+Ti+Nb atomic content lower than 5.15. In order to achieve higher strength this study has now been extended to higher S values. Nineteen compositions have been investigated (Fig.15) (Fig.15 and Table 2).

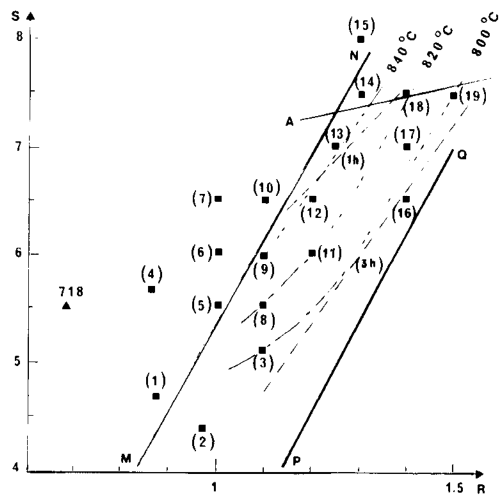

Figure 15 - Composition of the 19 investigated compositions in a S, R diagram. S = Ti + Al + Nb and R = Ti + Al/Nb are calculated using atomic percentage. The composition of Alloy 718 is also included.

Alloy	Mo	Ti	Al	Nb	Ta	S	R
1	2.80	0.72	0.63	4	-	4.70	0.89
2	7.0	0.59	0.63	3.41	-	4.24	0.97
3	7.0	0.90	0.74	3.85	-	5.14	1.11
4	6.1	0.89	0.70	3.50	2.4	5.67	0.87
5	3.0	0.86	0.80	4.43	-	5.50	1.00
6	3.0	0.93	0.88	4.83	-	6.00	1.00
7	3.0	1.01	0.95	5.22	-	6.50	1.00
8	3.0	0.90	0.84	4.23	-	5.50	1.10
9	3.0	0.98	0.92	4.60	-	6.00	1.10
10	3.0	1.06	1.00	4.99	-	6.50	1.10
11	3.0	1.04	0.96	4.37	-	6.00	1.20
12	3.0	1.11	1.04	4.77	-	6.50	1.20
13	3.0	1.21	1.14	5.02	-	7.00	1.25
14	3.0	1.32	1.24	5.26	-	7.50	1.30
15	3.0	1.41	1.33	5.61	-	8.00	1.30
16	3.0	1.18	1.11	4.38	-	6.50	1.40
17	3.0	1.28	1.20	4.72	-	7.00	1.40
18	3.0	1.37	1.28	5.06	-	7.50	1.40
19	3.0	1.41	1.32	4.85	-	7.50	1.50

Table 2 - Alloys compositions (Wt %). The parameters S = Ti + Al + Nb and R = Ti + Al/Nb have been calculated using atomic composition.

The combination of temperature (θ_o) and time (t_o) necessary to reach a critical size L_c (20 nm) for γ'' particles (Fig.14) were determined. The results are given in Fig.15 in a S-versus R diagram. In this figure the line AB represents an upper bound for the alloying elements above which it was found that the heats were difficult to be forged. The lines MN, PQ define a band within which the compact morphology could be formed. Corresponding heat treatments (temperature and time) are shown. In this diagram we have also reported a typical composition of the nominal Alloy 718 indicating that the compact morphology cannot be achieved in this material. Fig.16 shows that the increase in Al+Ti+Nb content enables to achieve both the compact morphology and attractive hardness values. More complete mechanical testing have been performed on these alloys to determine the intermediate and high temperature properties of such alloys as Alloy 13. In this alloy which was given the following heat-treatment : 850°C - 1h, cooling at 50°C/hour followed by aging at 650°C for 16 hours, the yield strengths measured at 25°C, 550°C, 650°C, 700°C and 750°C, were 1153 MPa, 976 MPa, 962 MPa, 948 MPa and 863 MPa, respectively. To test the thermal stability of Alloy 13, this material was submitted to prolonged aging at 700°C. The hardness value (420 Vickers) did not significantly change even after exposure times as long as 550 hours.

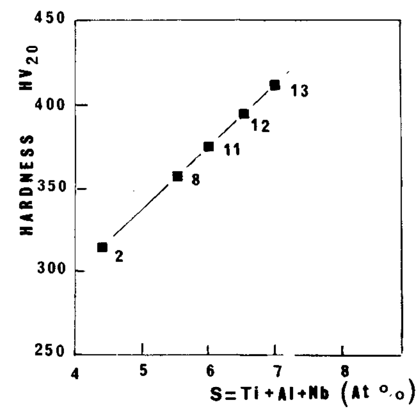

Figure 16 - Vickers hardness of 5 modified compositions leading to the compact morphology.

The summarize this section it can be stated that large improvements in the transgranular hardening of Alloy 718 can be effected. However these metallurgical developments must also be concerned with intergranular resistance which is the weakest link in this material as other Ni-base superalloys tested at elevated temperature.

Grain boundary strength

Grain size and grain boundary morphology. The elevated temperature behavior of Alloy 718 is strongly dependent on the details of the grain boundary morphology and of grain size. Fig.7 shows that the FCGR's measured under air environment with a hold time of 5 mn applied at maximum load were much lower in the necklace microstructure as compared to either large grain or small grain material. The results of creep crack growth rate measurements, shown in Fig.17, indicate that a similar behavior is observed

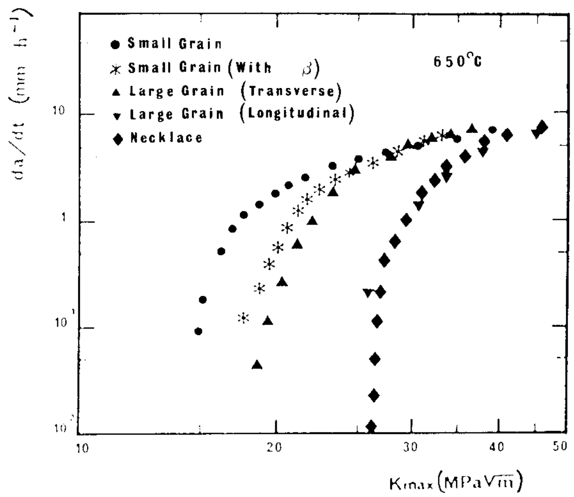

Figure 17 - Effect of grain size and grain boundary microstructure on the creep crack growth rate at 650°C [7].

when these microstructures were tested under sustained loading [7]. In this figure a strong effect of specimen orientation is also observed : the creep crack growth rates measured in specimens tested in the longitudinal direction, i.e. with a crack propagating along Nb carbides alignments are much larger than those determined in the perpendicular direction. The better resistance of the necklace microstructure was, in part, attributed to the fact that it facilitates crack branching effect [7] . This microstructure which consists of small recrystallized grains ($\simeq$ 5 µm) surrounding large warm-worked grains ($\simeq$ 150 µm) might also provide a crack tip shielding effect to oxygen penetration along the grain boundaries. Fig.17 shows also that, in small grain material ($\simeq$ 40 µm), the presence of β precipitates along the grain boundaries leads to an improvement in creep crack growth resistance. Similar results have been published recently [29]. This beneficial influence of β phase might also be related to grain boundary oxidation behavior either because of the intrinsic oxidation resistance of Ni_3 Nb phase or because of the existence of oxygen traps formed along the β interfaces.

Grain boundary chemistry. The grain boundary chemistry of Alloy 718 might also largely influence the elevated temperature properties, in particular the oxidation-assisted crack growth resistance. In this regard it is worth mentioning the work, essentially done in China, which showed that Mg addition raises not only high temperature tensile and stress-rupture ductilities but also increases smooth and notch stress-rupture life [30]. These modifications in mechanical properties were associated with a change in the fracture mode; Mg addition tends to improve the resistance to intergranular fracture. The basis role of Mg segregated at grain boundaries is not yet fully understood. Xie et al [30] suggested that the addition of this element leads to a change in the grain boundary β phase morphology by adopting a more globular and discrete from. This change is beneficial, as indicated previously. However one can also assume that Mg segregated at grain boundaries could play a more fundamental role in modifying the mechanism of intergranular oxidation, i.e. modifying the nature of the oxide film and controlling the oxygen penetration rate along the grain boundaries and the β interface. This idea, which is very speculative, deserves much further work.

Conclusions

Two aspects of the high temperature crack growth resistance of Alloy 718 have been examined :

(1) Oxidation-assisted crack growth

(i) Oxidation under air environment occurs in two stages, with the formation of a Ni,Fe rich oxide followed by that of the more protective film formed by Cr_2O_3 oxide. Under atmospheric pressure the transition time, t_p, between these two stages is of the order of a few minutes.

(ii) Although the details of grain boundary oxidation mechanisms are not yet fully understood it is suggested that transient effects observed in crack growth experiments, as well as the detrimental effect of hold time applied at minimum load in fatigue crack propagation tests, could be related to the existence of this transition time, t_p, between both types of oxides, the formation of Cr_2O_3 oxide leading to a "passivation" effect.

(iii) This form of chemical damage is reinforced by slip-induced intergranular cracking associated with the strong planar slip character of Alloy 718.

(iv) Much more experimental and theoretical work must be done before the firm conclusion is reached that the elevated temperature crack growth data are intrinsic and that they are not partially dependent on the experimental procedures as well as specimen preparation.

(2) Material improvement

(i) There is still a great potential for improving the elevated temperature properties of Alloy 718 by :

- major chemistry modifications. A close control of the (Ti+Al/Nb) ratio and of the (Ti+Al+Nb) sum is necessary to develop precipitate microstructures much more stable at elevated temperature. The requirements to achieve a specific γ', γ'' microstructure, the "compact morphology", are given for large variations in chemical composition.
- minor compositional modifications, such as Mg addition.
- control of the grain size and grain boundary microstructure.

(ii) The understanding and the improvement of the crack growth resistance of Alloy 718 must rely upon a better knowledge of the detrimental effect of oxidation.

Acknowledgments

The authors would like to acknowledge Dr. J.P. Pédron, Dr. J. Charpigny and Dr. A. Diboine former research students at the Centre des Matériaux Ecole des Mines de Paris. Thanks also to Pr. H. Ghonem presently on sabbatical leave from Rhode Island University (USA) for fruitful discussions during the preparation of this paper.

References

1. L.A. James, Fatigue crack propagation in Alloy 718 : A review. This conference.

2. P. Shahinian, H.E. Watson and H.H. Smith, J. Materials, (1972), p.527.

3. M.O. Speidel, Fatigue Crack Growth at High Temperatures, in "High Temperature Materials in Gas Turbines", edited by P.R. Sahm and M.O. Speidel, Elsevier Publishing Co., Amsterdam, (1974), p.207.

4. L.A. James, Fatigue Crack Propagation behavior of Inconel 718, HEDL Rep TME 75-80, Hanford Engineering Development Laboratory, Westinghouse Hanford Company, Richland, WA, September 1975.

5. W.J. Mills and L.A. James, ASME Publ. 78-WA/PVP-3, American Society of Mechanical Engineers, New York, 1978.

6. M. Clavel and A. Pineau, Mat. Sci. and Eng., 55, (1982), p.157-171 and 173-180.

7. J.P. Pédron and A. Pineau, Mat. Sci. and Engineering, 56, (1982), p.143-156.

8. P. Shahinian and K. Sadananda, Creep Fatigue Interactions, Proc. ASME Meet., American Society of Mechanical Engineers, New York, 1976, p.365.

9. P. Shahinian and K. Sadananda, J. Eng. Mat. Tech., 101, (1979), p.224.

10. A. Pineau, Intergranular Creep-Fatigue crack growth in Ni base alloys in "Flow and Fracture at Elevated Temperatures", edited by R. Raj, ASM (1983), 317-348.

11. A. Pineau, Elevated Temperature Life Predictions Methods and Mechanisms of Creep-Fatigue Interactions. NATO ASI "Advances in Fatigue Science and Technology". Alvor, Algarve, (Portugal), 22-15 April 1988. To appear.

12. A. Pineau, Elevated Temperature Creep-Fatigue Cracking in Relation to Oxidation Effects in ASM/NACE/AIME International Conference on Environment-Induced Cracking of Metals, 2-7 October 1988, Kohler, Wisconsin (USA). To appear.

13. L.C. Lim, R. Raj. On slip-induced intergranular cavitation during low cycle fatigue of nickel at intermediate temperature, Acta Metall., 32, (1984), p.727.

14. L.C. Lim and R. Raj. Effect of boundary structure on slip induced cavitation in polycristalline nickel, Acta Metall., 32, (1984), p.1183.

15. L.C. Lim. Surface intergranular cracking in large strain fatigue. Acta Metall., 35, (1987), p.1653.

16. D. Fournier and A. Pineau, Low Cycle Fatigue Behavior of Inconel 718 at 298K and 823K. Metall. Trans., 8A, (1977), 1095-1105.

17. M. Clavel and A. Pineau, Frequency and Wave-form Effects on the Fatigue Crack Growth Rate Behavior of Alloy 718 at 298K and 823K. Metall. Trans., 9A, (1978), 471-480.

18. M. Clavel, C. Levaillant and A. Pineau. Influence of micromechanisms of cyclic deformation at elevated temperature on fatigue behavior in "creep-Fatigue-Environment Interactions", edited by R.M. Pelloux and N.S. Stoloff. AIME Publication (1980), 24-45.

19. J.M. Oblak, D.S. Duvall and D.F. Paulonis. Metall. Trans., 5, (1974), p.143.

20. T.H. Sanders, R.E. Frischnuth and G.T. Embley. Metall. Trans., 12A, (1981), p.1003.

21. M. Sundararaman, P. Mukhopadhyay and S. Banerjee. Deformation behaviour of γ" strengthened Inconel 718. Acta Metall.,36, (1988), 847-864.

22. E. Andrieu, Influence de l'environnement sur la propagation des fissures dans un superalliage base Nickel : Inconel 718. Thesis Ecole des Mines (Paris), 22 Jan. 1987.

23. A. Diboine and A. Pineau, Creep crack initiation and growth in Inconel 718 alloy at 650°C. Fatigue Fracture Engineering Mater. Structures, 10, (1987), 141-151.

24. D.J. Wilson, J. Eng. Mater. Tech. Series H, 95, (1973), p.112.

25. R. Cozar and A. Pineau, Morphology of γ' and γ" precipitates and thermal stability of Inconel 718 Type alloys. Metall. Trans., 4A, (1973), 47-59.

26. M. Clavel, D. Fournier and A. Pineau. Plastic zone sizes in fatigued specimens of Inco 718. Metall. Trans., 6A, (1975), 2305-2307.

27. J.P. Collier, S.H. Wong, J.C. Phillips and J.K. Tien, The effect of varying Al, Ti and Nb content on the phase stability of Inconel 718. Metall. Trans., 19A, (1988), 1657-1666.

28. J.P. Collier, A.O. Selius and J.K. Tien. On developing a microstructurally and thermally stable iron-nickel base superalloy, in Superalloys 1988, edited by Q.S. Ruchman et al, (1988), 43-52.

29. A.K. Koul, P. Au, N. Bellinger, R. Thamburaj, W. Wallace and J.P. Immarigeon. Development of a damage tolerant microstructure for Inconel 718 turbine disc material; in Superalloys, edited by S. Reichman et al, (1988), 3-10.

30. X. Xie, Z. Xu, B.Qu, G. Chen and J.F. Radavich. The role of Mg on structure and mechanical properties in Alloy 718; in Superalloys 1988, edited by S. Reichman et al, (1988), 635-642.